

## 16. BIG-BANG NUCLEOSYNTHESIS

Revised September 1999 by K.A. Olive (Univ. of Minnesota).

Among the successes of the standard big-bang model is the agreement between the predictions of big-bang nucleosynthesis (BBN) for the abundances of the light elements, D,  $^3\text{He}$ ,  $^4\text{He}$ , and  $^7\text{Li}$ , and the primordial abundances inferred from observational data (see [1–4] for a more complete discussion). These abundances span some nine orders of magnitude:  $^4\text{He}$  has an abundance by number relative to hydrogen of about 0.08 (accounting for about 25% of the baryonic mass), while  $^7\text{Li}$ , the least abundant of the elements with a big-bang origin, has an abundance by number relative to hydrogen of about  $\sim 10^{-10}$ .

### 16.1. Big-bang nucleosynthesis theory

The BBN theory matches the observationally determined abundances with a single well-defined parameter, the baryon-to-photon ratio,  $\eta$ . All the light-element abundances can be explained with  $\eta$  in the range  $(1.2\text{--}5.7) \times 10^{-10}$ , or  $\eta_{10} \equiv \eta \times 10^{10} = 1.2\text{--}5.7$ . Equivalently, this range can be expressed as the allowed range for the baryon mass density,  $\rho_B = 0.8\text{--}3.9 \times 10^{-31} \text{ g cm}^{-3}$ , and can be converted to the fraction,  $\Omega$ , of the critical density,  $\rho_c$ .

The synthesis of the light elements was affected by conditions in the early Universe at temperatures  $T \lesssim 1 \text{ MeV}$ , corresponding to an age as early as 1 s. At somewhat higher temperatures, weak-interaction rates were in equilibrium, thus fixing the ratio of the neutron and proton number densities. At  $T \gg 1 \text{ MeV}$ ,  $n/p \approx 1$ , since the ratio was given approximately by the Saha relation,  $n/p \approx e^{-Q/T}$ , where  $Q$  is the neutron-proton mass difference. As the temperature fell, the Universe approached the point (“freeze-out”) where the weak-interaction rates were no longer fast enough to maintain equilibrium. The final abundance of  $^4\text{He}$  is very sensitive to the  $n/p$  ratio at freeze-out.

The nucleosynthesis chain begins with the formation of deuterium in the process  $pn \rightarrow D\gamma$ . However, photo-dissociation by the high number density of photons ( $n_\gamma/n_B = \eta^{-1} \sim 10^{10}$ ) delays production of deuterium (and other complex nuclei) well past the point where  $T$  reaches the binding energy of deuterium,  $E_B = 2.2 \text{ MeV}$ . (The average photon energy in a blackbody is  $\bar{E}_\gamma \approx 2.7 T$ .) When the quantity  $\eta^{-1} \exp(-E_B/T)$  reaches about 1 (at  $T \approx 0.1 \text{ MeV}$ ), the photo-dissociation rate finally falls below the nuclear production rate.

The 25% fraction of mass in  $^4\text{He}$  due to BBN is easily estimated by counting the number of neutrons present when nucleosynthesis begins. When the weak-interaction rates freeze-out at about  $T \approx 0.8 \text{ MeV}$ , the  $n$ -to- $p$  ratio is about 1/6. When free-neutron decays prior to deuterium formation are taken into account, the ratio drops to  $n/p \lesssim 1/7$ . Then simple counting yields a primordial  $^4\text{He}$  mass fraction

$$Y_p = \frac{2(n/p)}{1+n/p} \lesssim 0.25. \quad (16.1)$$

In the Standard Model, the  $^4\text{He}$  mass fraction depends primarily on the baryon-to-photon ratio  $\eta$ , as it is this quantity that determines when nucleosynthesis via deuterium production may begin. But because the  $n/p$  ratio depends only weakly on  $\eta$ , the  $^4\text{He}$  mass fraction is relatively flat as a function of  $\eta$ . The effect of the uncertainty in the neutron half-life,  $\tau_n = 886.7 \pm 1.9 \text{ s}$ , is now small. Lesser amounts of the other light elements are produced: D and  $^3\text{He}$  at the level of a few times  $10^{-5}$  by number relative to H, and  $^7\text{Li}/\text{H}$  at the level of about  $10^{-10}$ , when  $\eta$  is in the range  $1 - 10 \times 10^{-10}$ .

When we go beyond the Standard Model, the  $^4\text{He}$  abundance is very sensitive to changes in the expansion rate, which can be related to the effective number of neutrino flavors. This will be discussed below.

The calculated abundances of the light elements are shown in Fig. 16.1 as a function of  $\eta_{10}$ . The curves for the  $^4\text{He}$  mass fraction,  $Y_p$ , bracket the range based primarily on the uncertainty of the neutron mean-life. The spread in the  $^7\text{Li}$  curves is due to the  $1\sigma$  uncertainties in nuclear cross sections leading to  $^7\text{Li}$  and  $^7\text{Be}$  which subsequently decays to  $^7\text{Li}$  [5–7]. Similarly, the spread in the curves for D and  $^3\text{He}$  are  $1\sigma$  uncertainties in the D and  $^3\text{He}$  predictions. The

boxes show the observed abundances with their range of uncertainty, discussed below. Since the observational boxes line up on top of each other, there is an overall agreement between theory and observations for  $\eta_{10}$  in the range 1.2–5.7.

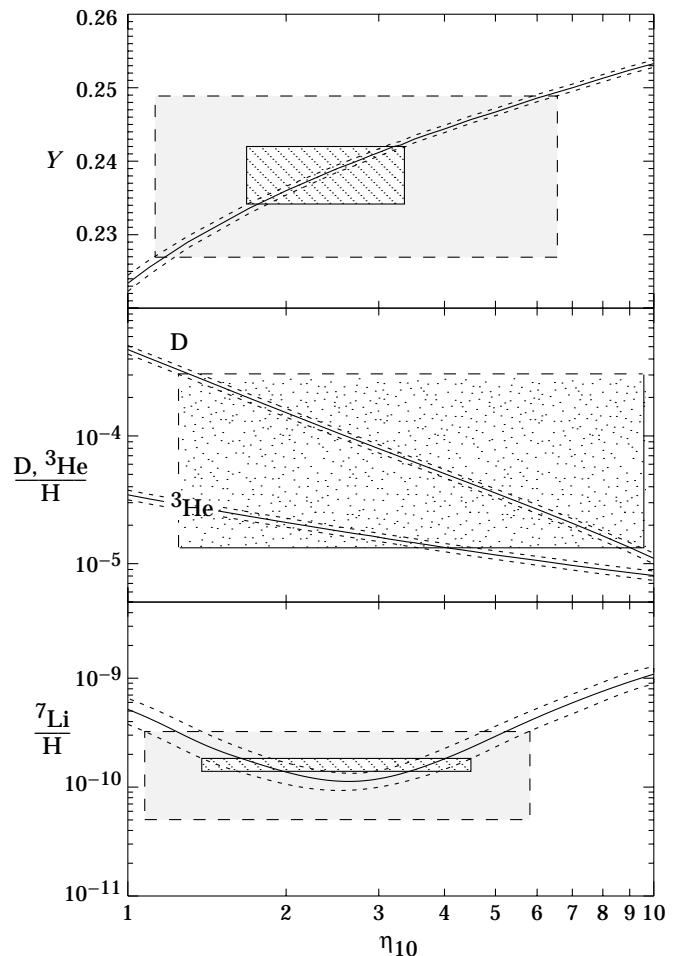


**Figure 16.1:** The abundances of D,  $^3\text{He}$ ,  $^4\text{He}$  and  $^7\text{Li}$  as predicted by the standard model of big-bang nucleosynthesis. Also shown by a series of boxes is the comparison between these predictions and the observational determination of the light element abundances. See text for details.

### 16.2. Observations

Because stars produce helium as well as heavier elements, one must search for primordial helium in regions where stellar processing has been minimal, *i.e.*, in regions where abundances of elements such as carbon, nitrogen and oxygen are very low. There are extensive compilations of observed abundances of  $^4\text{He}$ , N, and O in many different extra-galactic regions of ionized H [8,9]. Extrapolating the  $^4\text{He}$  abundances from the data leads to an observational estimate for  $Y_p$  of [10–13]

$$Y_p = 0.238 \pm 0.002 \pm 0.005. \quad (16.2)$$

(Here and elsewhere, the first error is the statistical standard deviation, and the second systematic.) The box in Fig. 16.1 bracketing the  $^4\text{He}$  curves covers the range 0.234–0.242, where the half height is given as twice the statistical error. Of course the real uncertainty is dominated by systematic effects and the dashed box is obtained using a larger error (twice the statistical and systematic error when added in quadrature) allowing  $Y_p$  to take values in an extended range 0.227–0.249.

Observations for deuterium and  $^3\text{He}$  abundances currently present certain difficulties. All deuterium is primordial [14], but some of the primordial deuterium has been destroyed. Thus, as can be seen in the figure, the present deuterium abundance gives us an absolute upper limit to  $\eta$ . However, to get more information requires either an understanding of galactic chemical evolution of deuterium or a direct measurement of primordial deuterium. Even more problematical is  $^3\text{He}$ : Not only is primordial  $^3\text{He}$  destroyed in stars but it is very likely that at least some low-mass stars are net producers of  $^3\text{He}$ . Neither the galactic chemical evolution of  $^3\text{He}$  nor the production of  $^3\text{He}$  in stars is well understood with standard models and observations presenting an inconsistent picture.

It appears that D/H has decreased over the age of the galaxy. Samples obtained deep inside meteorites provide measurements of the true (pre)-solar system abundance of  $^3\text{He}$ , while measurements on meteoritic near-surface samples, the solar wind, and lunar soil samples also contain  $^3\text{He}$  converted from deuterium in the early pre-main-sequence stage of the sun. The best current values are [15]

$$\begin{aligned} \left(\frac{\text{D} + ^3\text{He}}{\text{H}}\right)_{\odot} &= (4.1 \pm 1.0) \times 10^{-5}, \\ \left(\frac{^3\text{He}}{\text{H}}\right)_{\odot} &= (1.5 \pm 0.3) \times 10^{-5}. \end{aligned} \quad (16.3)$$

The difference between these, is the pre-solar D abundance. There has also been a recent measurement of HD in the atmosphere of Jupiter [16] yielding a value  $\text{D}/\text{H} = (2.7 \pm 0.7) \times 10^{-5}$  which is consistent with the above presolar value of D/H.

The present interstellar-medium abundance of D/H is [17]

$$\text{D}/\text{H} = 1.60 \pm 0.09_{-0.10}^{+0.05} \times 10^{-5}. \quad (16.4)$$

It is this lowest value of D/H that provides the most robust upper bound on  $\eta$ , since D is only destroyed. It is shown (decreased by twice the errors added in quadrature) as the lower right corner of the D and  $^3\text{He}$  box in Fig. 16.1. Thus, with confidence we can be sure that  $\eta_{10} < 9.5$  and correspondingly  $\Omega_B h^2 < 0.035$ .

Deuterium has also been detected in high-redshift, low-metallicity quasar absorption systems [18–20]. These measured abundances should represent the primordial value, but, they are at present not consistent: Two [18,19] give a relatively high value for  $\text{D}/\text{H} \approx 2 \times 10^{-4}$  while another two [20] give  $\text{D}/\text{H} \approx 3.4 \pm 0.3 \times 10^{-5}$ . Although it appears that the quality of the low D/H data is better than those showing high D/H, the latter can be used at the very least as an upper limit to primordial D/H and this is shown by the dashed box in Fig. 16.1, taking a  $2\sigma$  upper limit of  $\text{D}/\text{H} < 3 \times 10^{-4}$ . As one can see, the corresponding value of  $Y_p$  (at the same value of  $\eta$  as inferred by the observation of a high D/H) is in good agreement with the data.  $^7\text{Li}$  is also in agreement at this value as well. However, due to the still somewhat preliminary status of this observation, it is premature to use it to fix the primordial abundance. A high value for the D abundance would require an even greater degree of D destruction over the age of the galaxy. The lower measurement for D/H requires that systematics work coherently for both  $^4\text{He}$  and  $^7\text{Li}$  to give an overlap with this data. Systematic effects [21] may, however, imply a higher D/H abundance (in the low D/H objects) which is in the range  $3.5\text{--}5 \times 10^{-5}$ . At the upper end of this range, all of the light element abundances are also in concordance. Eventually, the primordial D/H issue will hopefully be resolved and give a correspondingly narrow allowed range in  $\eta$  and perhaps change the nature of the  $^3\text{He}$  and  $^7\text{Li}$  (see below) arguments which are currently dominated by galactic and/or stellar evolution issues.

Finally, we turn to  $^7\text{Li}$ . In old, hot, population-II stars,  $^7\text{Li}$  is found to have a very nearly uniform abundance. For stars with a surface temperature  $T > 5500$  K and a metallicity less than about 1/20th solar (so that effects such as stellar convection may not be important), the abundances show little or no dispersion beyond that consistent with the errors of individual measurements. Much data has been obtained recently from a variety of sources, and the best estimate for the mean  $^7\text{Li}$  abundance and its statistical uncertainty in halo stars

is [22] (the estimate of the systematic uncertainty discussed below is our own)

$$\text{Li}/\text{H} = (1.6 \pm 0.1_{-0.3}^{+0.4+0.9}) \times 10^{-10}. \quad (16.5)$$

The first error is statistical. The box in Fig. 16.1 corresponds to a  $2\sigma_{\text{stat}}$  spread. The second set of errors is a systematic uncertainty that covers the range of abundances derived by various methods. The third set of errors in Eq. (16.5) accounts for the possibility that some of the primordial  $^7\text{Li}$  has been destroyed in stars, and that as much as 40% of the observed  $^7\text{Li}$  was produced in cosmic ray collisions rather than in the Big Bang. This uncertainty has been constrained by recent observations showing some evidence for evolution in  $^7\text{Li}$  [23]. These uncertainties (depicted with a half height of  $2\sigma_{\text{stat}} + \sigma_{\text{syst}}$ ) are shown by the dashed box in Fig. 16.1. Observations of  $^6\text{Li}$ , Be, and B help constrain the degree to which these effects play a role [24–26].

### 16.3. A consistent value for $\eta$

For the Standard Model of BBN to be deemed successful, theory and observation of the light element abundances must agree using a single value of  $\eta$ . We summarize the constraints on  $\eta$  from each of the light elements. From the  $^4\text{He}$  mass fraction,  $Y_p < (0.242\text{--}0.249)$ , we have  $\eta_{10} < (3.4\text{--}6.6)$  as a  $2\sigma$  upper limit (the highest values use possible systematic errors as shown by the shaded box in the figure). Because of the sensitivity to the assumed upper limit on  $Y_p$  and Li/H, the upper limit on  $\eta$  from D/H, is still of value. From  $\text{D}/\text{H} > 1.3 \times 10^{-5}$ , we have  $\eta_{10} \lesssim 9.5$ .

The lower limit on  $\eta_{10}$  can be obtained from either D/H or  $^7\text{Li}$ . From the high D/H measurement in quasar absorption systems, we obtain  $\eta_{10} > 1.2$ .  $^7\text{Li}$  allows a broad range for  $\eta_{10}$  consistent with the other elements. When uncertainties in the reaction rates and systematic uncertainties in the observed abundances are both taken into account,  $^7\text{Li}$  allows values of  $\eta_{10}$  between (1.1–5.7).

The determination of  $\eta$  depends on our certainty that the observations of the light elements abundances can be translated into primordial abundances. This is perhaps more straightforward for  $^4\text{He}$  and  $^7\text{Li}$ , where the element abundances are determined in primitive low metallicity environments. If it turns out that a consistent value for D/H can be obtained from quasar absorption systems, then because of the slope of D/H with respect to  $\eta$ , D/H will be the best isotope for the determination of  $\eta$ . Until then, the use of the D and  $^3\text{He}$  abundance determinations is necessarily complicated by the evolution of the abundances of these elements over the star forming history of the galaxy. Uncertainties in the  $^3\text{He}$  evolution are compounded by uncertainties of stellar production/destruction mechanisms. The resulting overall consistent range for  $\eta_{10}$  is extended to (1.2–5.7) when systematic errors are pushed to their limits. These bounds on  $\eta_{10}$  constrain the fraction of critical density in baryons,  $\Omega_B$ , to be

$$0.004 < \Omega_B h_0^2 < 0.021. \quad (16.6)$$

For a Hubble parameter,  $h_0$ , between 0.4 and 1.0, the corresponding range for  $\Omega_B$  is 0.004–0.13.

Perhaps the best test of BBN will come when anisotropies in the microwave background check the determination of  $\Omega_B$ . At present, other measurements (such as of hot X-ray gas in clusters of galaxies, Lyman- $\alpha$  clouds, or microwave anisotropies) of  $\Omega_B$  give considerably larger uncertainties than those from BBN, but they are consistent with the BBN range.

### 16.4. Beyond the Standard Model

Limits on particle physics beyond the Standard Model come mainly from the observational bounds on the  $^4\text{He}$  abundance. As discussed earlier, the neutron-to-proton ratio is fixed by its equilibrium value at the freeze-out of the weak-interaction rates at a temperature  $T_f \sim 1$  MeV, with corrections for free neutron decay. Furthermore, freeze-out is determined by the competition between the weak-interaction rates and the expansion rate of the Universe,

$$G_F^2 T_f^5 \sim \Gamma_{\text{wk}}(T_f) = H(T_f) \sim \sqrt{G_N N} T_f^2, \quad (16.7)$$

where  $N$  counts the total (equivalent) number of relativistic particle species. The presence of additional neutrino flavors (or of any other relativistic species) at the time of nucleosynthesis increases the energy density of the Universe and hence the expansion rate, leading to a larger value of  $T_f$ ,  $n/p$ , and ultimately  $Y_p$ . It is clear that just as one can place limits [27] on  $N$ , any changes in the weak or gravitational coupling constants can be similarly constrained.

In the Standard Model, the number of particle species can be written as  $N = 5.5 + \frac{7}{4}N_\nu$ ; 5.5 accounts for photons and  $e^\pm$ , and  $N_\nu$  is the number of (massless) neutrino flavors. The helium curves in Fig. 16.1 were computed assuming  $N_\nu = 3$ , and the computed  ${}^4\text{He}$  abundance scales roughly as  $\Delta Y_{\text{BBN}} \approx 0.012 - 0.014 \Delta N_\nu$ . Clearly the central value for  $N_\nu$  from BBN will depend on  $\eta$ . If the best value for the observed primordial  ${}^4\text{He}$  abundance is 0.238, then, for  $\eta_{10} \sim 1.8$ , the central value for  $N_\nu$  is very close to 3. By means of a likelihood analysis on  $\eta$  and  $N_\nu$  based on  ${}^4\text{He}$  and  ${}^7\text{Li}$  [28,29] (see also [30]) it was found that the 95% CL ranges are  $1.7 \leq N_\nu \leq 4.3$ , and  $1.4 \leq \eta \leq 4.9$ .

The limits on  $N_\nu$  can be translated into limits on other types of particles or particle masses that would affect the expansion rate of the Universe just prior to nucleosynthesis. In some cases, it is the interaction strengths of new particles which are constrained. Particles with less than full weak strength interactions contribute less to the energy density than particles that remain in equilibrium up to the time of nucleosynthesis [31].

We close with a simple example. Suppose there exist three right-handed neutrinos with only right-handed interactions of strength  $G_R < G_F$ . The standard left-handed neutrinos are no longer in equilibrium at temperatures below  $\sim 1$  MeV. Particles with weaker interactions decouple at higher temperatures, and their number density ( $\propto T^3$ ) relative to neutrinos is reduced by the annihilations of particles more massive than 1 MeV. If we use the upper bound  $N_\nu < 4.0$ , then the three right-handed neutrinos must have a temperature  $3(T_{\nu_R}/T_{\nu_L})^4 < 1$ . Since the temperature of the decoupled  $\nu_R$ 's is determined by entropy conservation,  $T_{\nu_R}/T_{\nu_L} = [(43/4)/N(T_f)]^{1/3} < 0.76$ , where  $T_f$  is the freeze-out temperature of the  $\nu_R$ 's. Thus  $N(T_f) > 24$  and decoupling must have occurred at  $T_f > 140$  MeV. Finally, the decoupling temperature is related to  $G_R$  by  $(G_R/G_F)^2 \sim (T_f/3 \text{ MeV})^{-3}$ , where 3 MeV corresponds to the decoupling temperature for  $\nu_L$ . This yields a limit  $G_R \lesssim 10^{-2} G_F$ . These limits are strongly dependent on the assumed upper limit to  $N_\nu$ ; for  $N_\nu < 3.5$ , the limit on  $G_R$  strengthened to  $G_R < 0.002 G_F$ , since  $T_f$  is constrained to be larger than the temperature corresponding to the QCD transition in the early Universe.

#### References:

1. D.N. Schramm and R.V. Wagoner, *Ann. Rev. Nucl. and Part. Sci.* **27**, 37 (1977).
2. A. Boesgard and G. Steigman, *Ann. Rev. Astron. Astrophys.* **23**, 319 (1985).
3. T.P. Walker, G. Steigman, D.N. Schramm, K.A. Olive, and H.-S. Kang, *Astrophys. J.* **376**, 51 (1991).
4. K.A. Olive, G. Steigman, and T.P. Walker, *Phys. Rep.* (in press) astro-ph/9905320.
5. C.J. Copi, D.N. Schramm, and M.S. Turner, *Science* **267**, 192 (1995).
6. L.M. Krauss and P. Romanelli, *Astrophys. J.* **358**, 47 (1990).
7. N. Hata, R.J. Scherrer, G. Steigman, D. Thomas, and T.P. Walker, *Astrophys. J.* **458**, 637 (1996).
8. B.E.J. Pagel, E.A. Simonson, R.J. Terlevich, and M. Edmunds, *MNRAS* **255**, 325 (1992).
9. Y.I. Izotov, T.X. Thuan, and V.A. Lipovetsky, *Astrophys. J.* **435**, 647 (1994);  
Y.I. Izotov and T.X. Thuan, *Astrophys. J. Supp.* **108**, 1 (1997);  
*Astrophys. J.* **500**, 188 (1998).
10. K.A. Olive and G. Steigman, *Astrophys. J. Supp.* **97**, 49 (1995).
11. K.A. Olive and S.T. Scully, *Int. J. Mod. Phys. A* **11**, 409 (1996).
12. K.A. Olive, E. Skillman, and G. Steigman, *Astrophys. J.* **493**, 788 (1997).
13. B.D. Fields and K.A. Olive, *Astrophys. J.* **506**, 177 (1998).
14. H. Reeves, J. Audouze, W. Fowler, and D.N. Schramm, *Astrophys. J.* **179**, 909 (1973).
15. J. Geiss, in *Origin and Evolution of the Elements*, eds. N. Prantzos, E. Vangioni-Flam, and M. Cassé (Cambridge: Cambridge University Press, 1993), p. 89.
16. H.B. Niemann *et al.*, *Science*, 272, 846 (1996);  
P.R. Mahaffy *et al.*, *Sp. Sci. Rev.* **84**, 251 (1998).
17. J.L. Linsky, *et al.*, *Astrophys. J.* **402**, 695 (1993);  
J.L. Linsky, *et al.*, *Astrophys. J.* **451**, 335 (1995).
18. R.F. Carswell, M. Rauch, R.J. Weymann, A.J. Cooke, J.K. Webb, *MNRAS* **268**, L1 (1994);  
A. Songaila, L.L. Cowie, C. Hogan, M. Rugers, *Nature* **368**, 599 (1994).
19. J.K. Webb *et al.*, *Nature* **388**, 250 (1997);  
D. Tytler *et al.*, *Astron. J.* **117**, 63 (1999).
20. D. Tytler, X.-M. Fan, and S. Burles, *Nature* **381**, 207 (1996);  
D. Tytler, and S. Burles, *Astrophys. J.* **460**, 584 (1996);  
D. Tytler, and S. Burles, *Astrophys. J.* **499**, 699 (1998);  
D. Tytler, and S. Burles, *Astrophys. J.* **507**, 732 (1998).
21. S. Levshakov, D. Tytler, and S. Burles, astro-ph/9812114.
22. P. Molaro, F. Primas, and P. Bonifacio, *Astron. & Astrophys.* **295**, L47 (1995);  
P. Bonifacio and P. Molaro, *MNRAS*, 285,847(1997).
23. S.G. Ryan, J.E. Norris, and T.C. Beers, *Astrophys. J.* (in press) astro-ph/9903059 (1999).
24. T.P. Walker, G. Steigman, D.N. Schramm, K.A. Olive, and B. Fields, *Astrophys. J.* **413**, 562 (1993).
25. K.A. Olive, and D.N. Schramm, *Nature* **360**, 439 (1993).
26. G. Steigman, B. Fields, K.A. Olive, D.N. Schramm, and T.P. Walker, *Astrophys. J.* **415**, L35 (1993);  
E. Vangioni-Flam *et al.*, *New Astronomy* **4**, 245 (1999);  
B.D. Fields and K.A. Olive, *New Astronomy* **4**, 255 (1999).
27. G. Steigman, D.N. Schramm, and J. Gunn, *Phys. Lett.* **B66**, 202 (1977).
28. B.D. Fields and K.A. Olive, *Phys. Lett.* **B368**, 103 (1996);  
B.D. Fields, K. Kainulainen, D. Thomas, and K.A. Olive, *New Astronomy* **1**, 77 (1996).
29. K.A. Olive and D. Thomas, *Astro. Part. Phys.* **7**, 27 (1997);  
K.A. Olive and D. Thomas, *Astro. Part. Phys.* **11**, 403 (1999).
30. C.J. Copi, D.N. Schramm, and M.S. Turner, *Phys. Rev.* **D55**, 3389 (1997).
31. G. Steigman, K.A. Olive, and D.N. Schramm, *Phys. Rev. Lett.* **43**, 239 (1979);  
K.A. Olive, D.N. Schramm, and G. Steigman, *Nucl. Phys.* **B180**, 497 (1981).